Massive glycosaminoglycan-dependent entry of Trp-containing cell-penetrating peptides induced by exogenous sphingomyelinase or cholesterol depletion.

Chérine Bechara, Manjula Pallerla, Fabienne Burlina, Françoise Illien, Sophie Cribier, Sandrine Sagan

Massive glycosaminoglycan-dependent entry of Trp-containing cell-penetrating peptides induced by exogenous sphingomyelinase or cholesterol depletion

Chérine Bechara[a,b,c,#], Manjula Pallerla[a,b,c], Fabienne Burlina[a,b,c], Françoise Illien[a,b,c], Sophie Cribier[a,b,c] and Sandrine Sagan[*a,b,c.] [a] Sorbonne Universités, UPMC Univ Paris 06, LBM, 4 Place Jussieu, F-75005, Paris, France, [b] Ecole Normale Supérieure-PSL Research University, Département de Chimie, 24, rue Lhomond, 75005 Paris, France, [c] CNRS, UMR 7203 LBM, F-75005, Paris, France.

*** Corresponding author:** Sandrine Sagan (PhD), Université Pierre et Marie Curie, Laboratoire des Biomolécules, UMR 7203 CNRS-ENS, cc182, 4 place Jussieu, 75252 Paris cedex 05, France, Phone: +33 1 44 27 38 42, Fax: +33 1 44 27 71 50, sandrine.sagan@upmc.fr,

Abstract

Among non-invasive cell delivery strategies, cell-penetrating peptide (CPP) vectors represent interesting new tools. To get fundamental knowledge about the still debated internalisation mechanisms of these peptides, we modified the membrane content of cells, typically by hydrolysis of sphingomyelin or depletion of cholesterol from the membrane outer leaflet. We quantified and visualised the effect of these viable cell-surface treatments on the internalisation efficiency of different CPPs, among which the most studied Tat, R_9, penetratin and analogues, that all carry the N-terminal biotin-Gly_4 tag cargo. Under these cell membrane treatments, only penetratin and R_6W_3 underwent a massive glycosaminoglycan (GAG)-dependent entry in cells. Internalization of the other peptides was only slightly increased, similarly in the absence or the presence of GAGs for R_9, and only in the presence of GAGs for Tat and R_6L_3. Ceramide formation (or cholesterol-depletion) is known to lead to the reorganisation of membrane lipid domains into larger platforms, which can serve as a trap and cluster receptors. These results show that GAG-clustering, enhanced by formation of ceramide, is efficiently exploited by penetratin and R_6W_3, which contain Trp residues in their sequence but not Tat, R_9 and R_6L_3. Hence, these data shed new lights on the differences in the internalisation mechanism and pathway of these peptides that are widely used in delivery of cargo molecules.

Ceramide-enriched domain / endocytosis / tryptophan-rich peptide / arginine-rich peptide / cationic peptide

[#] Present address: University of Oxford, Department of Chemistry, Chemistry Research Laboratory cherine.bechara@chem.ox.ac.uk,

Introduction

Ever since their discovery two decades ago, extensive studies are carried out in order to understand the mechanisms of cellular internalisation of cell-penetrating peptides (CPPs) [1-3]. These are short peptides (5-30 residues), generally cationic, that have the capacity to cross cell membranes in a non-invasive way and can thus be used to deliver various cargoes, including therapeutics, inside living cells [4-6]. However, the final cellular localisation depends on the internalisation mechanism of the conjugated CPP-cargo conjugates, which stresses the importance of understanding their internalisation pathways.

For all the described mechanisms of CPP internalization (endocytosis and direct translocation), cell entry must involve as a first step interaction with the plasma membrane (PM) bilayer. The latter has a very complex and dynamic structure, where the lateral organisation and segregation play a major role in trafficking processes, mainly through lipid rafts [7,8]. These rafts are reported as highly dynamic transient microdomains enriched in cholesterol and sphingomyelin (SM) in the outer leaflet of the PM, and thought to cluster into larger platforms in response to specific stimuli [8]. The implication of lipid rafts in the internalisation of CPPs in different cell lines was mostly studied by using various inhibitors of lipid raft-dependent endocytosis (mainly via cholesterol depletion) or by following different markers that would be sorted in such domains [9-13]. However, few are the studies that have assessed the implication of the SM/cholesterol interactions and the resulting PM organisation during internalisation. It was demonstrated that CPPs are taken up into mammalian cells more efficiently than into plant protoplast [14], probably because of the difference in sterol lipids and the absence of SM in plant cell membranes compared to mammalian PM. Moreover, the well-known CPP penetratin was shown to induce negative curvature, important for translocation, in fluid membrane domains but not in raft-like domains [15], while adding cholesterol to DOPG/DOPC vesicles was shown to increase the binding affinity of different analogues of penetratin to large unilamellar vesicles (LUVs) without evidence for specific peptide/cholesterol interactions [16]. A recent study suggested that high concentrations (> 15 µM) of some CPP sequences enhance internalisation by triggering the translocation of intracellular acid sphingomyelinase (SMase) from the cytosol to the outer leaflet of the plasma membrane, where it hydrolyses SM and produces ceramide-enriched domains [17].

In the present work, we explored the role of the two components of membrane microdomains, SM and cholesterol, on CPP internalisation in living cells, in the presence or absence of cell-surface glycosaminoglycans (GAGs). In fact, GAGs are present in the ectodomains of proteoglycans, which can be localised in cholesterol and SM-enriched plasma membrane microdomains. GAGs serve as high capacity regions for concentrating positively charged CPPs, and then transferring them to outer membrane lipids, or can directly internalise CPPs through clustering [18-20]. A recent study suggested that multivalent Tat peptide induces heparan sulfate proteoglycans clustering and recruitment to actin-associated lipid rafts, thus causing its internalisation by macropinocytosis [21].

To obtain basic knowledge about the internalisation mechanisms, we modified the membrane content of cells, typically by hydrolysis of sphingomyelin or depletion of cholesterol. The tested peptides were all modified at the N-terminus with a biotinyl-Gly_4 bait and quantitation tag sequence, which can be assimilated as a cargo moiety identical for all CPP sequences. We used five different CPPs (Table 1) -Tat, penetratin, R_9, R_6W_3 and R_6L_3 - and quantified the effect of these cell-surface treatments on their internalisation in a mutant GAG-deficient cell line (CHO-pgsA745, GAG^{neg}) compared to wild-type CHO (WT) cells. This GAG-deficient cell line has been widely employed before to analyse the impact of GAGs on the internalisation efficiency of various permeant molecules, and not only CPPs. It has been characterised both genetically (defect in xylosyltransferase) and biochemically (90-95 % GAG-deficient phenotype) [22] and is known to feature almost abolished endocytosis pathways for CPPs [23-26]. Thus we examined whether the effects of SMase or MβCD treatments are different when cells express different levels of cell-surface GAGs. The effect of SM hydrolysis was also visualised using confocal laser scanning microscopy for two representative CPPs, Tat peptide and penetratin. Further on, the effect of cholesterol depletion on the internalisation of these two CPPs was also studied, and their interaction with model systems mimicking lipid rafts was quantified. In this study, we have used peptide concentrations ranging from 1 µM up to 30 µM. One reason is that different internalisation pathways are involved according to the peptide concentration [24]. GAG-dependent internalization of penetratin is indeed activated at higher micromolar peptide concentration (> 3 µM) than for translocation [24]. The second reason is that some CPPs activate endogenous SMase release above 20µM extracellular concentration [17]. This peptide concentration is high for delivery purposes, but local membrane concentrations could reach that value with accumulation of the peptide at the vicinity of the membrane after peptide administration *in vivo*.

Materials and Methods

Materials - Peptides (containing N-terminal biotin-G4 moiety and carboxamide at C-terminus) were obtained from PolyPeptide Laboratories (Strasbourg, France) or synthesized using the Boc-solid phase strategy. POPC and POPG were obtained as a powder from Genzyme (Switzerland). Cholesterol was purchased from Avanti Polar Lipids (Alabaster, AL). Ceramide, TRITC-streptavidin and avidin were purchased from ZYMED

laboratories (Invitrogen). Anti-ceramide mouse IgM was purchased from Glycobiotech (Borstel, Germany) and anti-Mouse IgG from Jackson Immunoresearch Labs. Phalloidin-FITC, neutral sphingomyelinase from *Bacillus cereus*, heparinase I, heparinase III and chondroitinase ABC, methyl-β-cyclodextrin (MβCD), chicken egg yolk sphingomyelin (Fluka), FITC-dextran (4.4 kDa and 70 kDa) and all other reagents were from Sigma-Aldrich.

Cell culture - Wild type Chinese Hamster Ovary CHO-K1 cells (WT) and xylose transferase- or GAG-deficient CHO-pgsA745 cells (GAG^{neg}) were obtained from the American Type Culture Collection (Rockville, MD). All cell lines were grown in Dulbecco's modified Eagle's medium (DMEM) supplemented with 10% fetal calf serum (FCS), penicillin (100,000 IU/L), streptomycin (100,000 IU/L), and amphotericin B (1 mg/L) in a humidified atmosphere containing 5 % CO_2 at 37 °C.

Quantification of the internalised peptide - 10^6 cells in suspension were incubated with 5 mM MβCD for 30 min at 37 °C. Cells were then washed with 1mL HBSS, then incubated with the peptide [biotinyl-(^{1}H)G_4 tagged] at the indicated concentration in 1 mL total DMEM volume for 70 min at 37 °C. Cells were treated with trypsin before their lysis in the presence of a known amount of the [biotinyl-(^{2}H)G_4 tagged] internal standard peptide. Capture of the (^{1}H)- and (^{2}H)-labelled peptides was carried out with streptavidin-coated magnetic beads. The amount of internalised peptide (captured on beads) was then quantified by matrix-assisted laser desorption/ ionisation-Time of flight mass spectrometry (MALDI-TOF MS) as described [27,28]. To be accurate, quantification of the internalisation requires working with an identical number of cells upon different experimental conditions. Adherent cells are easier to handle. However upon MβCD treatment, we observed that some cells detached from the wells, without induced toxicity. Since washing steps are required for the preparation of the samples for MALDI-MS based quantifications (by direct aspiration of the buffered solution for adherent cells, or centrifugation steps to recover cells in suspension), we chose to perform internalisation with cells in suspension to avoid loosing the detached cells. By contrast, in the case of SMase treatment, cells did not detach. Therefore, 10^6 adherent cells were incubated with the peptides [biotinyl-(^{1}H)G_4 tagged] at the indicated concentrations in the presence of 1U/ml of neutral SMase from *Bacillus cereus*, in 1 mL total DMEM volume for 70 min at 37 °C. To remove cell-surface GAGs, cells were incubated for 45 min at 37°C in Hank's Balanced Salt Solution with heparinase I, heparinase III and chondroitinase ABC (every enzyme at 0.1 U/ 10^6 cells /ml). Cells were washed and further incubated in the presence of penetratin (10 µM) with or without SMase (1U/ml). The amount of internalised peptide was then quantified as described above. Experiments were repeated independently at least three times in triplicates.

Ceramide quantification in cells by flow cytometry - Cells were detached from the culture plate with 0.5 mM EDTA in PBS (5 min at 37°C). One million cells in suspension were incubated in the presence or absence of 0.05 U of SMase in 200 µL DMEM for 30 min at 37°C. After washings by centrifugation (800g, 5 min, 4°C), cells were fixed in 3 % paraformaldehyde (4 °C, 10 min) and incubated with 10% FCS in PBS (20 °C, 30 min). Cells were incubated with a mouse anti-ceramide IGM antibody (1µg/ml) for 1h at room temperature. After PBS washes, cells were incubated with a secondary FITC-labeled anti-mouse antibody (SIGMA, 5µg/ml)) for 1h at room temperature, then washed and kept in PBS for the flow cytometry analysis (FACS Calibur flow cytometer (BD Biosciences) using 488 nm laser excitation and a 515-545 nm emission filter. Each sample was analyzed for 10 000 events. The mean fluorescence values were obtained by subtracting the mean fluorescence without anti-ceramide antibody from the mean fluorescence of cells.

Fluorescence microscopy - 10^5 cells were cultured, a day before, on cover slips in 24-well plates in DMEM supplemented with 10% FCS. After washing with culture medium, cells were incubated for 40 min with the biotinylated peptides at 37 °C, in the presence or absence of 0.05 U of SMase in 200 mL DMEM. Cells were washed three times with cold medium and incubated with unlabeled avidin (10 µM) to block the membrane-bound peptide before fixation [29]. After washings, cells were fixed in 3 % paraformaldehyde (4 °C, 10 min), permeabilised with 0.1% TX-100 in phosphate- buffered saline (20 °C, 5 min) and incubated with 10% FCS in phosphate-buffered saline (20 °C, 30 min). Biotinylated peptides were detected with streptavidin-TRITC (2 µg/ml) for 1h at room temperature. Cells were then incubated with phalloidin-fluorescein isothiocyanate (1/1000) (Sigma) for 30 min at room temperature, and finally incubated with DAPI (1.5 µg/ml) (Pierce) for 10 min at room temperature. Cover slips were mounted in Fluoromount mounting medium for observation by confocal microscopy on an inverted Leica DMI 6000. Experiments were repeated several times for consistency and gave identical results.

Cell viability assays – Effects of SMase or MßCD on cell viability was evaluated with CCK8 kit (Dojindo Laboratoiries). Briefly 25,000-30,000 WT and GAG^{neg} cells were seeded into 96 multiwell plates 24h before cell viability assays. The culture medium (with FCS) was replaced by culture medium (without FCS) without (control) or with SMase or MßCD at the indicated concentrations and CCK8. Cells were incubated for 75 min to

130 min at 37°C before OD (450 nm and reference at 620 nm) measurement (PolarStar, BMG Labtech). The concentrations of SMase and MβCD were chosen to incorporate those used in MS quantification and imaging experiments. Data result from two independent experiments in triplicates.

Liposome preparation - Lipid films were made by dissolving lipids into chloroform or a mixture of chloroform and methanol (4/1 vol/vol). The solvent was then evaporated using a rotary evaporator and the dissolving/evaporation step was repeated three times. Lipid films were then hydrated with 50 mM Tris-Cl, 2 mM EDTA, 150 mM NaCl, pH 7.5. The films were then vortexed extensively at a temperature superior to the one of phase transition temperature of the lipid to obtain multilamellar vesicles (MLVs). To form LUVs, the MLVs were subjected to five freeze/thawing cycles. The homogeneous lipid suspension was passed 19 times through a mini-extruder (Avanti Alabaster, AL) equipped with two stacked 100 nm polycarbonate membranes.

Isothermal titration calorimetry experiments - ITC experiments were performed on a TA Instrument nano ITC calorimeter. Titrations were performed by injecting 10 µL aliquots of peptide solutions (concentration between 250 and 500 µM) into the calorimeter cell containing 10 mg/ml LUVs, with 10 min injection intervals. The experiments were performed at 25 °C, a temperature at which vesicles are in fluid phase. Data analysis was performed with the NanoAnalyse software provided by TA Instruments.

Results

Boosting the internalisation efficiency of Trp-containing CPPs upon sphingomyelin hydrolysis in the outer membrane leaflet of cells

Quantification of the internalised peptide - One convenient method for depletion of SM from cell membrane surfaces consists in their treatment with exogenous SMase. SM is then converted into ceramide, this leads to the accumulation of this latter, which alters the surface topography by enhancing membrane curvature [30] as well as inducing phase separation and formation of condensed ceramide-enriched domains [31,32]. We tested the effect of SM hydrolysis on the entry efficiency of CPPs into two model cell lines, WT and GAG^{neg} CHO cells, the latter being chosen to examine in addition the role of proteoglycans. The peptides were used at different extracellular concentrations: penetratin, R_6W_3, R_6L_3, R_9 and Tat peptide (Table 1). We quantified by MALDI-TOF MS the amount of internalised peptide after 70 min incubation (plateau of the internalisation kinetics) with one million cells, in the presence or absence of SMase (Figure 1). It should be noted that treatment of both cell types with SMase at the concentration used to study CPP internalization by MS (1 U SMase / mL / one million cells) did not induce any cytotoxic effect (Supplementary figure 1).

In WT cells, the internalisation of all CPPs increased upon SMase treatment but the effect was quantitatively different according to the peptide sequence and concentration. A strong increase in the amount of internalisation was measured for R_6W_3 (12-fold for 10 µM extracellular peptide concentration) and penetratin (4, 6 and 8 fold increase for 1, 10 and 30 µM extracellular peptide concentration, respectively). The effect was less important (2 to 3 fold) for R_9 (10 and 30 µM), R_6L_3 and Tat. Interestingly, the impact of SM hydrolysis on the internalisation of R_6W_3 and penetratin was lower in GAG^{neg} cells. A 2-fold increase in internalisation was observed for R_6W_3 (10 µM), whereas for penetratin an effect was observed only at high peptide concentration (3-fold increase at 30 µM). On the other hand, there was a 2-fold increase in the internalisation of R_9 (10 and 30 µM) but no effect of SMase treatment on the internalisation of Tat and R_6L_3. As mentioned before, SMase treatment did not perturb viability of WT and GAG^{neg} cells, discarding cytotoxicity as an explanation for the boosting effect of SMase on penetratin and R_6W_3 entry observed especially in WT cells. To confirm the direct implication of GAGs in the massive internalization observed for the two CPPs, penetratin and R_6W_3, we studied on penetratin whether an enzymatic removal of cell-surface carbohydrates before SMase treatment gave similar results as those obtained with GAG^{neg} cells. As shown in Table 2, the effect of SMase on penetratin internalization was similar in WT cells treated with a combination of heparinase I, heparinase III and chondroitinase ABC and GAG^{neg}, confirming the direct involvement of GAGs in the massive internalization of the peptide.

Thus, SMase treatment induced massive GAG-dependent endocytosis of penetratin and R_6W_3, while for R_9 the effect was similar in WT and GAG^{neg} cells, suggesting that SMase-mediated higher uptake of R_9 is independent of the presence of GAGs. Finally, the internalisation of Tat and R_6L_3 was weakly affected by SM hydrolysis and only in WT cells, suggesting that GAG-dependent endocytosis was slightly enhanced in this case.

Fluorescence staining - Because the major effect of SMase on peptide entry was measured in the presence of GAGs, we examined by confocal microscopy the internalisation, in WT and GAG^{neg} CHO cells, of two of the peptides that behaved differently: penetratin and Tat. In parallel, formation of ceramide was detected with monoclonal anti-ceramide antibodies, and quantified by flow cytometry (Figure 2) in non-permeabilised and fixed cells (Supplementary figure 2). As expected, treatment of cells with SMase increased the specific anti-ceramide antibody staining of the cell-surface from the two cell lines. Interestingly, ceramide-staining was

mostly punctuated with big patches visible at the cell-surface of the two cell types (Supplementary figure 2B, 2D) compared to the control (Supplementary figure 2A, 2C), a relevant indication of the segregation of ceramide-enriched membrane domains. Flow cytometry (Figure 2) showed that ceramide production was even more important in GAG^{neg} compared to WT cells after 30 minutes SMase treatment. This observation likely results from the presence of GAGs at the cell-surface of WT compared to GAG^{neg} cells that should impede access of SMase to the lipid bilayer.

Consistent with the massive increased intracellular peptide quantity measured by MALDI-MS, a massive penetratin staining (cytosol and nuclei) was visible inside some WT cells (Figure 3B, upper, and Supplementary figure 3) upon SMase treatment, compared to control cells (Figure 3A, and Supplementary figure 3). Furthermore, in the absence of the massive peptide staining, we could clearly detect punctuations starting from the plasma membrane (nucleation zones) and visible till the nucleus (Figure 3B). In the case of Tat peptide (Figure 4A, 4B, and Supplementary figure 4) we never observed a massive staining, but few cells presented nucleation zones on the plasma membrane (Figure 4B).

On the other hand, in GAG^{neg} cells the cytoplasmic fluorescent signal of penetratin staining became more punctuated upon SM hydrolysis (Figure 3D) compared to untreated cells (Figure 3C). As for Tat, we could not visualise any difference in the staining, in the presence or the absence of SMase (Figure 4C, 4D). Finally, at higher extracellular concentrations of penetratin (30 µM), the number of WT cells presenting massive staining upon SM hydrolysis was significantly higher (Supplementary figure 5). More interestingly, stress fibers of actin cytoskeleton were also much more visible (Supplementary figure 5). We could also detect an increase in the fluorescence staining of the peptide in GAG^{neg} cells, sometimes with visible nucleation zones (Supplementary figure 6).

GAG-dependent endocytosis of penetratin and R_6W_3 is different from pinocytosis

Altogether, the latter results show that the higher penetratin and R_6W_3 internalisation in WT cells compared to GAG^{neg} cells following SM hydrolysis more likely corresponds to a boosting effect of endocytic processes dependent on the presence of cell-surface GAGs. Because it was previously reported that GAG clustering might be related to activation of macropinocytosis [33], we wanted to verify whether this is the case for these cell-penetrating peptides.

Therefore, the selective role of GAGs in the massive internalisation of penetratin and R_6W_3 was further examined for two chemically unrelated general endocytosis markers: FM1-43 for plasma membrane labeling, and FITC-Dextran (4.4 kDa) as a bulk marker. Unlike CPPs, FM1-43 and FITC-Dextran showed similar enhancement of internalisation during SM hydrolysis in both cell lines (Supplementary figure 7). In particular, labelling of cells with the bulk marker FITC-Dextran was massive in all WT and GAG^{neg} cells. Furthermore, the addition of any of the five CPPs (10 µM) did not change the intensity and distribution of the endocytic markers, be it with or without SMase treatment. Similar results were obtained with FITC-Dextran of higher molecular weight (70 kDa). These results show that the entry pathway of penetratin and R_6W_3 in WT cells, is selectively driven by the presence of GAGs and is likely distinct from macropinocytosis and general endocytosis.

We further tested this hypothesis by analysing if the internalisation in WT cells of a low-efficient CPP, R_6L_3, could be affected by the co-presence of the highly efficient analogue R_6W_3. The high efficiency of internalisation of R_6W_3 was indeed found related to its high binding affinity for heparin and chondroitin sulfate and its propensity to induce GAG clustering, in contrast to R_6L_3 entry which is not dependent on cells-surface GAGs [18] (Figure 1). After incubation of cells for 5-15 min with R_6L_3 (10 µM) to allow its adsorption at the cell-surface, R_6W_3 (2 or 10 µM) was added, for additional 60 min incubation. For this experiment, only the R_6L_3 peptide contained a N-terminal biotin label to allow its capture with streptavidin-coated magnetic beads. Quantification of R_6L_3 in these conditions showed that the presence of R_6W_3 decreases the entry of R_6L_3 in cells. The presence of 2 µM R_6W_3 evoked a two-fold inhibition of the entry (0.15 ± 0.05 µM versus 0.30 ± 0.06 µM), while increasing the concentration of R_6W_3 to 10 µM prevented totally the intracellular detection of R_6L_3. These results support the idea that R_6W_3 GAG-dependent entry is an internalisation pathway that is distinct from bulk-phase pinocytosis (macropinocytosis), otherwise it would have stimulated or enhanced the entry of R_6L_3.

Cholesterol depletion enhances the internalisation of penetratin but not of Tat in the presence of cell-surface GAGs

Cholesterol strongly interacts with SM and is responsible for the formation of liquid-ordered (L_o) domains in the cell plasma membrane. These L_o plasma domains are implicated in various clathrin-independent endocytic routes. Partial removing of membrane cholesterol would thus be interesting to test the role of L_o domains in the entry of CPPs. A simple method for depleting cholesterol relies on its extraction with methyl-β-cyclodextrin (MβCD) [34]. Such MβCD treatments were previously reported to decrease the internalisation of Tat peptide [35] and penetratin [36], a result interpreted as the inhibition of raft-dependent endocytosis of these peptides [37,38].

Using MβCD, we found herein the necessity to wash this compound out before adding peptides to the cells. We measured indeed a decrease in Tat and penetratin internalisation in the presence of MβCD (2 to 3 fold less internalised peptides) compared to the quantity internalised in the absence of MβCD treatment. This decrease was not due to the inhibition of raft-dependent endocytosis but likely to the binding and entrapment of the peptides into the hydrophobic cavity of the sugar ring through the aromatic side-chains of Phe, Tyr and Trp amino acids as reported [39], which leads to depletion of the free peptide from the extracellular milieu. Rodal *et al*. previously reported that upon MβCD treatment the uptake of transferrin was still inhibited by ~20% after 1h incubation even when serum or cholesterol was added; total recovery of cholesterol in the plasma membrane was reached 3 hours after treatment with MβCD [40]. Thus, the experimental conditions we used were to incubate cells with MβCD, and to wash cells quickly before further incubation with CPPs. On the other hand, we compared the effect of MβCD treatment in WT and GAG^{neg} cells, both cell lines having similar quantities of plasma membrane cholesterol [41,42]. MβCD treatment of cells did not influence cell viability (supplementary figure 8).

Using this protocol for cholesterol depletion, there was no significant effect on the internalisation of penetratin at low micromolar extracellular concentration (1 μM) in WT and GAG^{neg} cells (Figure 4), a concentration at which the peptide directly translocates into cells and does not trigger GAG-dependent endocytosis [24,18]. However, at higher concentration of penetratin (10 μM), a 50% increase in its internalisation was quantified in WT cells, while there was no significant difference in its internalisation in GAG^{neg} cells. In contrast, there was no significant difference in the internalisation of Tat in both cell lines after MβCD treatment even at 10 μM extracellular peptide concentration. MβCD treatment has been associated to a fluidification of the PM and thus an increase in peptide translocation [12]. However, the fact that for penetratin we did not see the same effect in GAG^{neg} and WT cells indicates that its increased uptake upon MβCD treatment should be related to a GAG-dependent entry.

Binding of penetratin and Tat to LUVs mimicking cholesterol- and sphingomyelin-rich membrane domains

To further compare the interaction of the peptides with the membrane lipids, we measured the binding of penetratin and Tat peptide to large unilamellar vesicles (LUVs) mimicking cholesterol- and sphigomyelin-rich membrane domains, with or without additional ceramide. Various mixtures of cholesterol, SM, PC representative (1-palmitoyl-2-oleoyl-*sn*-glycero-3-phosphocholine (POPC)) and ceramide (N-palmitoylsphingosine, C_{16}-Ceramide) were used to form the liposomes [43]. PG (1-palmitoyl-2-oleoyl-*sn*-glycero-3-phosphoglycerol (POPG)) was added in small amounts (5% mole) as the single negatively charged lipid to minimise fusion of the vesicles. Control liposomes made of PC/PG (95/5) were also studied in interaction with the two peptides (Table 3). The binding constant measured by ITC is an apparent binding constant (K^{app}) reflecting three putative steps of the peptide binding to LUVs: adsorption of the peptide at the membrane surface (interaction with polar heads of phospholipids), hydrophobic penetration between fatty acyl chains and change of peptide conformation. Penetratin interacted better with LUVs mimicking rafts compared to pure PC/PG, and the presence of ceramide did not have any significant impact on the binding of the peptide to LUVs. As for Tat peptide, there was no difference between the interaction with the raft-like mixtures and pure PC/PG. But the binding of Tat increased deeply (~10 fold) in the presence of ceramide in the raft-like mixtures.

These results highlight the importance of both electrostatic and hydrophobic interactions in the binding of the peptides to lipid vesicles. Indeed, addition of ceramide to vesicles likely clustered or segregated the negatively charged PG, which increased the binding of Tat peptide (8 positive charges and no Trp) to the lipid vesicles. In the case of penetratin (7 positive charges and 2 Trp), the two tryptophans add a hydrophobic contribution to the interaction with LUVs, such that the global binding of the peptide did not change significantly in the presence or the absence of ceramide. These results also show that there is no direct relationship between the affinity of these peptides for ceramide-enriched membranes and their efficacy to internalise into cells.

Discussion

We found that SM hydrolysis (or ceramide generation) and cholesterol depletion in the cell plasma membrane increased the internalisation of cationic CPPs (Table 2). This increased efficiency of entry was much higher in cells containing chondroitin and heparan sulfate proteoglycans compared to cells depleted in these GAGs. This effect on the internalisation efficiency was also found higher for CPP sequences that contain tryptophan residues (penetratin and R_6W_3) compared to arginine-rich peptides with no tryptophan (R_9, Tat and R_6L_3) and confirmed previous results about the role of Trp in the interaction of peptides with GAGs [18].

The results also suggest that GAG-clustering is enhanced by conversion of SM into ceramide. Ceramide formation was proposed to lead to the reorganisation of membrane lipid domains into larger platforms, which could serve as a trap and cluster receptors [44,45]. For example, generation of ceramide through endogenous SMase action is used by some pathogens to enter host cells by receptor clustering [46]. Activation of

endogeneous SMase was also proposed as a way for cell-penetrating peptides to enter cells when used at high-concentrations [17].

Treatment of CHO cells with exogenous SMase has been found to induce rapid formation of endocytic vesicles, which are 400 nm in diameter and not enriched in clathrin or caveolin, and that pinch off from the plasma membrane and move into the cytosol [47]. Holopainen *et al.* attributed the endocytic budding vesicles to the tendency of ceramide to separate into domains and to form negative spontaneous curvature, leading to membrane invagination [48]. In this study, this mechanical energy-independent endocytosis (discussed below) was likely more visible in GAG^{neg} cells, for which it was no longer masked by the important effect of GAG clustering. SMase treatment induces lateral displacement of cholesterol in the plasma membrane of living cells (maximum depletion 60 min after the addition of SMase) [49-52], probably due to the formation of ceramide [53] and segregation of lipids. Following SMase treatment, recovery of cholesterol-rich plasma membrane domains is at the same rate as SM is resynthesized from ceramide (partial recovery 180 min after the addition of SMase) [51,52]. Hence, ceramide generation leads to the disruption of cholesterol-rich microdomains from the plasma membrane [54], making it somehow similar to the effect of depleting cholesterol. For instance, the increase in the internalisation of the cell-penetrating peptide $R_{8,}$ upon MβCD treatment had already been reported [12], and attributed to a fluidification of the plasma membrane leading to an increase in peptide translocation. We confirm herein this previous assumption, since similar boosting effect of SMase treatment was observed on R_9 entry into GAG^{neg} cells compared to WT cells, when R_9 entry in GAG^{neg} cells mostly relies on direct translocation across the cell membrane [24].

Cholesterol depletion induces aggregation of plasma membrane domains that contain signalling molecules and are involved in endocytosis and in actin polymerisation [55,56]. Thus, penetratin and R_6W_3 interact strongly with and cluster GAGs present in SM- and cholesterol-rich domains to induce endocytosis, a segregation process expected to be enhanced when the cell membrane is enriched in ceramide or depleted in cholesterol. Furthermore, our data support the idea that GAG-clustering and GAG-dependent endocytosis activated by these CPPs, is distinct from bulk-phase pinocytosis. Indeed upon SMase treatment we found similar entry of bulk phase endocytic markers in the two cell types. Moreover the concomitant incubation of a peptide that does not cluster GAGs (R_6L_3) with a high-efficient one (R_6W_3) [18], led to a decreased entry of the former. In the case of GAG-activated macropinocytosis it would have been expected that more R_6L_3 would have entered into cells.

On the other hand, in the absence of GAGs another route of entry is brought out, likely at the level of the lipid bilayer. We previously reported that in the absence of GAGs, the main route of entry of R_9, penetratin and R_6W_3 is direct translocation across the plasma membrane [18,24]. Herein, formation of ceramide-enriched domains also segregates and increases the clustering of charged lipids and thus the charge density in domains of the plasma membrane. In addition to this propensity to promote phase separation, ceramide is known to induce negative curvature and mechanical stress in membrane [57]. Hence R_9, penetratin and R_6W_3 could exploit the negative curvature induced by ceramide formation to evoke mechanical endocytosis as reported in membrane models for penetratin [15]. Concomitantly, CPP binding to cell membranes causes surface tension because of the perturbation of polar head groups and acyl chains packing of the lipid bilayer. Because of the physico-chemical properties of ceramide, the frequency of formation of defects is thereby enhanced when ceramide is produced in the membrane. The increased frequency of events such as membrane thinning and formation of defects in the bilayer [58], both decrease the energetic penalty necessary to form a transient pore that would allow translocation of the CPP inside cells, thanks to the membrane potential driving-force [59].

Conclusions

To conclude, considering the results obtained with SMase and with cholesterol-depletion, we propose a model for the effect of ceramide-generation on the internalisation of CPPs (Figure 5). An efficient cell-penetrating peptide would bind, recruit and cluster specific membrane lipids, and thus evoke, stabilise locally and exploit membrane thinning and defects to translocate. Alternatively, the CPP can bind and cluster GAGs that act as autonomous receptors and follow a specific endocytosis pathway whose mechanism remains to be fully understood [60, 61]. The kinetics of a given CPP to partition between cell-surface GAGs and in defect regions of the lipid bilayer would determine the balance between endocytosis and translocation pathways of internalisation.

Acknowledgements

Support for this research was provided by the Université Pierre et Marie Curie (UPMC; Sorbonne Universités), by ANR BLAN2010-ParaHP (postdoctoral position for M.P.), by the École Normale Supérieure (ENS), the Centre National de la Recherche Scientifique (CNRS), and the French Ministère de l'Enseignement Supérieur et de la Recherche (PhD fellowship for C.B.).

The authors declare that they have no conflict of interest.

References

1. Bechara C, Sagan S (2013) Cell-penetrating peptides: 20 years later, where do we stand? FEBS Letters 587 (12):1693-1702
2. Madani F, Lindberg S, Langel U, Futaki S, Graslund A (2011) Mechanisms of cellular uptake of cell-penetrating peptides. J Biophys 2011:414729
3. Jones AT, Sayers EJ (2012) Cell entry of cell penetrating peptides: tales of tails wagging dogs. J Control Release 161 (2):582-591
4. van den Berg A, Dowdy SF (2011) Protein transduction domain delivery of therapeutic macromolecules. Current opinion in biotechnology 22 (6):888-893
5. Said Hassane F, Saleh AF, Abes R, Gait MJ, Lebleu B (2010) Cell penetrating peptides: overview and applications to the delivery of oligonucleotides. Cell Mol Life Sci 67 (5):715-726
6. Jarver P, Mager I, Langel U (2010) In vivo biodistribution and efficacy of peptide mediated delivery. Trends in pharmacological sciences 31 (11):528-535
7. Anderson RG, Jacobson K (2002) A role for lipid shells in targeting proteins to caveolae, rafts, and other lipid domains. Science (New York, NY 296 (5574):1821-1825
8. Mayor S, Rao M (2004) Rafts: scale-dependent, active lipid organization at the cell surface. Traffic (Copenhagen, Denmark) 5 (4):231-240
9. Saalik P, Elmquist A, Hansen M, Padari K, Saar K, Viht K, Langel U, Pooga M (2004) Protein cargo delivery properties of cell-penetrating peptides. A comparative study. Bioconjugate chemistry 15 (6):1246-1253
10. Wadia JS, Stan RV, Dowdy SF (2004) Transducible TAT-HA fusogenic peptide enhances escape of TAT-fusion proteins after lipid raft macropinocytosis. Nature medicine 10 (3):310-315
11. Foerg C, Ziegler U, Fernandez-Carneado J, Giralt E, Rennert R, Beck-Sickinger AG, Merkle HP (2005) Decoding the entry of two novel cell-penetrating peptides in HeLa cells: lipid raft-mediated endocytosis and endosomal escape. Biochemistry 44 (1):72-81
12. Fretz MM, Penning NA, Al-Taei S, Futaki S, Takeuchi T, Nakase I, Storm G, Jones AT (2007) Temperature-concentration- and cholesterol-dependent translocation of L- and D-octa-arginine across the plasma and nuclear membrane of CD34+ leukaemia cells. The Biochemical journal 403 (2):335-342
13. Mager I, Langel K, Lehto T, Eiriksdottir E, Langel U (2012) The role of endocytosis on the uptake kinetics of luciferin-conjugated cell-penetrating peptides. Biochimica et biophysica acta 1818 (3):502-511
14. Mae M, Myrberg H, Jiang Y, Paves H, Valkna A, Langel U (2005) Internalisation of cell-penetrating peptides into tobacco protoplasts. Biochimica et biophysica acta 1669 (2):101-107
15. Lamaziere A, Wolf C, Lambert O, Chassaing G, Trugnan G, Ayala-Sanmartin J (2008) The homeodomain derived peptide Penetratin induces curvature of fluid membrane domains. PloS one 3 (4):e1938
16. Caesar CE, Esbjorner EK, Lincoln P, Norden B (2006) Membrane interactions of cell-penetrating peptides probed by tryptophan fluorescence and dichroism techniques: correlations of structure to cellular uptake. Biochemistry 45 (24):7682-7692
17. Verdurmen WP, Thanos M, Ruttekolk IR, Gulbins E, Brock R (2010) Cationic cell-penetrating peptides induce ceramide formation via acid sphingomyelinase: implications for uptake. J Control Release 147 (2):171-179
18. Bechara C, Pallerla M, Zaltsman Y, Burlina F, Alves ID, Lequin O, Sagan S (2013) Tryptophan within basic peptide sequences triggers glycosaminoglycan-dependent endocytosis. The FASEB Journal 27 (2):738-749
19. Poon GM, Gariepy J (2007) Cell-surface proteoglycans as molecular portals for cationic peptide and polymer entry into cells. Biochemical Society transactions 35 (Pt 4):788-793
20. Letoha T, Keller-Pinter A, Kusz E, Kolozsi C, Bozso Z, Toth G, Vizler C, Olah Z, Szilak L (2010) Cell-penetrating peptide exploited syndecans. Biochimica et biophysica acta 1798 (12):2258-2265
21. Imamura J, Suzuki Y, Gonda K, Roy CN, Gatanaga H, Ohuchi N, Higuchi H (2011) Single particle tracking confirms that multivalent Tat protein transduction domain-induced heparan sulfate proteoglycan cross-linkage activates Rac1 for internalization. The Journal of biological chemistry 286 (12):10581-10592
22. Esko JD, Stewart TE, Taylor WH (1985) Animal cell mutants defective in glycosaminoglycan biosynthesis. Proceedings of the National Academy of Sciences 82 (10):3197-3201
23. Marty C, Meylan C, Schott H, Ballmer-Hofer K, Schwendener RA (2004) Enhanced heparan sulfate proteoglycan-mediated uptake of cell-penetrating peptide-modified liposomes. CMLS, Cell Mol Life Sci 61 (14):1785-1794.
24. Jiao CY, Delaroche D, Burlina F, Alves ID, Chassaing G, Sagan S (2009) Translocation and endocytosis for cell-penetrating peptide internalization. The Journal of biological chemistry 284 (49):33957-33965
25. Amand HL, Rydberg HA, Fornander LH, Lincoln P, Norden B, Esbjorner EK (2012) Cell surface binding and uptake of arginine- and lysine-rich penetratin peptides in absence and presence of proteoglycans. Biochimica et biophysica acta 1818 (11):2669-2678
26. Gump JM, June RK, Dowdy SF (2010) Revised Role of Glycosaminoglycans in TAT Protein Transduction Domain-mediated Cellular Transduction. Journal of Biological Chemistry 285 (2):1500-1507.

27. Burlina F, Sagan S, Bolbach G, Chassaing G (2005) Quantification of the cellular uptake of cell-penetrating peptides by MALDI-TOF mass spectrometry. Angewandte Chemie (International ed 44 (27):4244-4247
28. Burlina F, Sagan S, Bolbach G, Chassaing G (2006) A direct approach to quantification of the cellular uptake of cell-penetrating peptides using MALDI-TOF mass spectrometry. Nature protocols 1 (1):200-205
29. Dupont E, Prochiantz A, Joliot A (2007) Identification of a Signal Peptide for Unconventional Secretion. Journal of Biological Chemistry 282 (12):8994-9000.
30. Mathivet L, Cribier S, Devaux PF (1996) Shape change and physical properties of giant phospholipid vesicles prepared in the presence of an AC electric field. Biophysical journal 70 (3):1112-1121
31. Holopainen JM, Subramanian M, Kinnunen PK (1998) Sphingomyelinase induces lipid microdomain formation in a fluid phosphatidylcholine/sphingomyelin membrane. Biochemistry 37 (50):17562-17570
32. Fanani ML, Hartel S, Oliveira RG, Maggio B (2002) Bidirectional control of sphingomyelinase activity and surface topography in lipid monolayers. Biophysical journal 83 (6):3416-3424
33. Lambaerts K, Wilcox-Adelman SA, Zimmermann P (2009) The signaling mechanisms of syndecan heparan sulfate proteoglycans. Current Opinion in Cell Biology 21 (5):662-669.
34. Hao M, Mukherjee S, Sun Y, Maxfield FR (2004) Effects of cholesterol depletion and increased lipid unsaturation on the properties of endocytic membranes. The Journal of Biological Chemistry 279 (14):14171-14178
35. Kaplan IM, Wadia JS, Dowdy SF (2005) Cationic TAT peptide transduction domain enters cells by macropinocytosis. J Control Release 102 (1):247-253
36. Letoha T, Gaal S, Somlai C, Venkei Z, Glavinas H, Kusz E, Duda E, Czajlik A, Petak F, Penke B (2005) Investigation of penetratin peptides. Part 2. In vitro uptake of penetratin and two of its derivatives. J Pept Sci 11 (12):805-811
37. Conner SD, Schmid SL (2003) Regulated portals of entry into the cell. Nature 422 (6927):37-44
38. Subtil A, Gaidarov I, Kobylarz K, Lampson MA, Keen JH, McGraw TE (1999) Acute cholesterol depletion inhibits clathrin-coated pit budding. Proceedings of the National Academy of Sciences of the United States of America 96 (12):6775-6780
39. Irie T, Uekama K (1999) Cyclodextrins in peptide and protein delivery. Advanced Drug Delivery Reviews 36 (1):101-123.
40. Rodal SK, Skretting G, Garred O, Vilhardt F, van Deurs B, Sandvig K (1999) Extraction of cholesterol with methyl-beta-cyclodextrin perturbs formation of clathrin-coated endocytic vesicles. Molecular biology of the cell 10 (4):961-974
41. Bishop JR, Stanford KI, Esko JD (2008) Heparan sulfate proteoglycans and triglyceride-rich lipoprotein metabolism. Current Opinion in Lipidology 19 (3):307-313
42. Bishop JR, Passos-Bueno MR, Fong L, Stanford KI, Gonzales JC, Yeh E, Young SG, Bensadoun A, Witztum JL, Esko JD, Moulton KS (2010) Deletion of the Basement Membrane Heparan Sulfate Proteoglycan Type XVIII Collagen Causes Hypertriglyceridemia in Mice and Humans. PloS one 5 (11):e13919
43. Veatch SL, Keller SL (2005) Miscibility phase diagrams of giant vesicles containing sphingomyelin. Physical review letters 94 (14):148101
44. Gulbins E, Grassme H (2002) Ceramide and cell death receptor clustering. Biochimica et biophysica acta 1585 (2-3):139-145
45. Gulbins E, Dreschers S, Wilker B, Grassme H (2004) Ceramide, membrane rafts and infections. Journal of molecular medicine (Berlin, Germany) 82 (6):357-363
46. Grassme H, Jendrossek V, Riehle A, von Kurthy G, Berger J, Schwarz H, Weller M, Kolesnick R, Gulbins E (2003) Host defense against Pseudomonas aeruginosa requires ceramide-rich membrane rafts. Nature medicine 9 (3):322-330
47. Zha X, Pierini LM, Leopold PL, Skiba PJ, Tabas I, Maxfield FR (1998) Sphingomyelinase treatment induces ATP-independent endocytosis. The Journal of cell biology 140 (1):39-47
48. Holopainen JM, Angelova MI, Kinnunen PK (2000) Vectorial budding of vesicles by asymmetrical enzymatic formation of ceramide in giant liposomes. Biophysical journal 78 (2):830-838
49. Chatterjee S (1994) Neutral sphingomyelinase action stimulates signal transduction of tumor necrosis factor-alpha in the synthesis of cholesteryl esters in human fibroblasts. The Journal of biological chemistry 269 (2):879-882
50. Ridgway ND (2000) Interactions between metabolism and intracellular distribution of cholesterol and sphingomyelin. Biochimica et biophysica acta 1484 (2-3):129-141
51. Ridgway ND, Lagace TA, Cook HW, Byers DM (1998) Differential effects of sphingomyelin hydrolysis and cholesterol transport on oxysterol-binding protein phosphorylation and Golgi localization. The Journal of biological chemistry 273 (47):31621-31628
52. Al-Makdissy N, Younsi M, Pierre S, Ziegler O, Donner M (2003) Sphingomyelin/cholesterol ratio: an important determinant of glucose transport mediated by GLUT-1 in 3T3-L1 preadipocytes. Cellular signalling 15 (11):1019-1030

53. Megha, London E (2004) Ceramide selectively displaces cholesterol from ordered lipid domains (rafts): implications for lipid raft structure and function. The Journal of biological chemistry 279 (11):9997-10004
54. Nyholm TK, Grandell PM, Westerlund B, Slotte JP (2010) Sterol affinity for bilayer membranes is affected by their ceramide content and the ceramide chain length. Biochimica et biophysica acta 1798 (5):1008-1013
55. Mahammad S, Dinic J, Adler J, Parmryd I (2010) Limited cholesterol depletion causes aggregation of plasma membrane lipid rafts inducing T cell activation. Biochimica et Biophysica Acta (BBA) - Molecular and Cell Biology of Lipids 1801 (6):625-634
56. Quinn PJ (2010) A lipid matrix model of membrane raft structure. Progress in Lipid Research 49 (4):390-406
57. López-Montero I, Monroy F, Vélez M, Devaux PF (2010) Ceramide: From lateral segregation to mechanical stress. Biochimica et Biophysica Acta (BBA) - Biomembranes 1798 (7):1348-1356
58. Last NB, Schlamadinger DE, Miranker AD (2013) A common landscape for membrane-active peptides. Protein Science 22 (7):870-882
59. Rothbard JB, Jessop TC, Lewis RS, Murray BA, Wender PA (2004) Role of Membrane Potential and Hydrogen Bonding in the Mechanism of Translocation of Guanidinium-Rich Peptides into Cells. Journal of the American Chemical Society 126 (31):9506-9507
60. Christianson HC, Belting M (2013) Heparan sulfate proteoglycan as a cell-surface endocytosis receptor. Matrix biology : journal of the International Society for Matrix Biology. pii: S0945-053X(13)00133-9
61. Christianson HC, Svensson KJ, van Kuppevelt TH, Li JP, Belting M (2013) Cancer cell exosomes depend on cell-surface heparan sulfate proteoglycans for their internalization and functional activity. Proc Natl Acad Sci U S A. 110(43):17380-17385

Table 1 - Sequence of the peptides (biotin-Gly_4 at the N-terminus, carboxamide at the C-terminus) used in this study. Net positive charge (*Z*), number of arginine $n_{(R)}$ and tryptophan residues $n_{(W)}$.

Peptide	Sequence	*Z*	$n_{(R)}$	$n_{(W)}$
R_9	RRRRRRRRR	+9	9	0
Tat(47-57)	YGRKKRRQRRR	+8	6	0
R_6L_3	RRLLRRLRR	+6	6	0
Penetratin	RQIKIWFQNRRMKWKK	+7	3	2
R_6W_3	RRWWRRWRR	+6	6	3

Table 2 – Impact of cell-surface treatment on internalization of CPPs in wild type and GAG^{neg} cells – Cells were incubated with 10 μM peptide. Data are normalized for every peptide to the quantity measured in control wild-type cells**.** SMase, sphingomyelinase; HI, heparinase I; HIII, heparinase III; ChABC, chondroitinase ABC.

Peptide	Wild-type				GAG-deficient		
	SMase	HI, HIII, ChABC	SMase, HI, HIII, ChABC	MβCD	control	SMase	MβCD
R_6L_3	2	-	-	-	1	1	-
Tat	3	-	-	1	1	1	1
R_9	3	-	-	-	0.35	0.65	-
penetratin	6	0.75	0.71	2	0.60	0.40	1
R_6W_3	8	-	-	-	0.70	1.35	-

Table 3 - Binding of penetratin and Tat peptide to LUVs of different lipid content. PC/PG: 95/5 mol%; Chol/SM/PC/PG: 20/50/25/5 mol%; Chol/SM/Cer/PC/PG: 20/40/10/25/5. Chol, cholesterol; Cer, ceramide. For calculation of K^{app}, it was assumed that 50% of the total lipids were accessible to the peptide in LUV.

	K^{app} (μM)	
Lipid mixture	Penetratin	Tat
PC/PG	9.0 ± 5.0	12 ± 7.5
Chol/SM/PC/PG	2.7 ± 0.5	10 ± 0.3
Chol/SM/Cer/PC/PG	1.7 ± 1.1	0.8 ± 0.2

Figure legends

Figure 1: Quantification of the internalisation of the CPPs, studied in the presence and the absence of SMase, in WT and GAG^{neg} cells at 37 °C. 10^6 cells were incubated with the peptides in the presence or the absence of 1U SMase, in 1 mL DMEM, at 37 °C for 70 min. The amounts of internalised peptides (µM) were then quantified using a MALDI-TOF MS reported protocol[27,28]. Experiments were done in duplicate or triplicate, and repeated at least three times independently. Significance was tested using a Welch's corrected t test (ns $p>0.05$, * $0.05<p>0.01$, ** $0.01<p>0.001$, *** $p<0.001$).

Figure 2: Ceramide quantification upon sphingomyelinase treatment of (A) WT cells or (B) GAG^{neg} cells. 10^6 cells in suspension were incubated with or without 0.05 U SMase at 37 °C for 30 min. Fixed cells were then labeled with anti-ceramide (1mg/ml) mouse IgM and FITC-labeled anti-mouse IgM. Experiments were done in triplicate. Significance was provided using a Kolmorov-Smirnov test: (A) D = 0.43, (B) D = 0.92.

Figure 3: Confocal microscopy of penetratin internalisation (10 µM extracellular concentration) in WT cells in the absence (A) and the presence (B) of SMase, and in GAG^{neg} cells in the absence (C) and the presence (D) of SMase. The peptide is labeled in red (streptavidin-TRITC), the actin cytoskeleton protein in green (phalloidin-FITC) and the cell nuclei in blue (DAPI). Scale bar corresponds to 10 µm. Unmerged pictures are shown in Supplementary figure 3.

Figure 4: Confocal microscopy of Tat peptide internalisation (10 µM extracellular concentration) in WT cells in the absence (A) and the presence (B) of SMase, and in GAG^{neg} cells in the absence (C) and the presence (D) of SMase. The peptide is labeled in red (streptavidin-TRITC), the actin cytoskeleton protein in green (phalloidin-FITC) and the cell nuclei in blue (DAPI). Scale corresponds to 10 µm. Unmerged pictures are shown in Supplementary figure 4.

Figure 5: Quantification of the internalisation of penetratin and Tat peptide in the presence and the absence of MβCD, in WT and GAG^{neg} cells at 37 °C. 10^6 cells were incubated with 5 mM MβCD at 37 °C for 30 min, cells were washed then incubated with the different peptides in 1 mL DMEM, at 37 °C for 70 min. The amounts of internalised peptides (µM) were then quantified using a MALDI-TOF MS protocol [27,28]. Experiments were done in duplicate or triplicate, and repeated at least three times independently. Significance was tested using a Welch's corrected t test (ns $p>0.05$, * $0.05<p>0.01$, ** $0.01<p>0.001$, *** $p<0.001$).

Figure 6: Proposed mechanism for the enhanced internalisation of CPPs due to ceramide-enriched domain formation. The positively charged peptides interact with the negatively charged lipids and GAGs on the cell surface. SMase hydrolyses extracellular leaflet SM, present in lipid rafts, which causes the generation of ceramide-enriched domains. This enhances clustering and subsequent endocytosis of GAGs, which is massive in the case of tryptophan-containing basic CPPs. On the other hand, arginine-rich CPPs can translocate directly into the cytoplasm at the defective interfaces between ceramide-enriched domains and the bulk of the plasma membrane.

Figure 1
Click here to download high resolution image

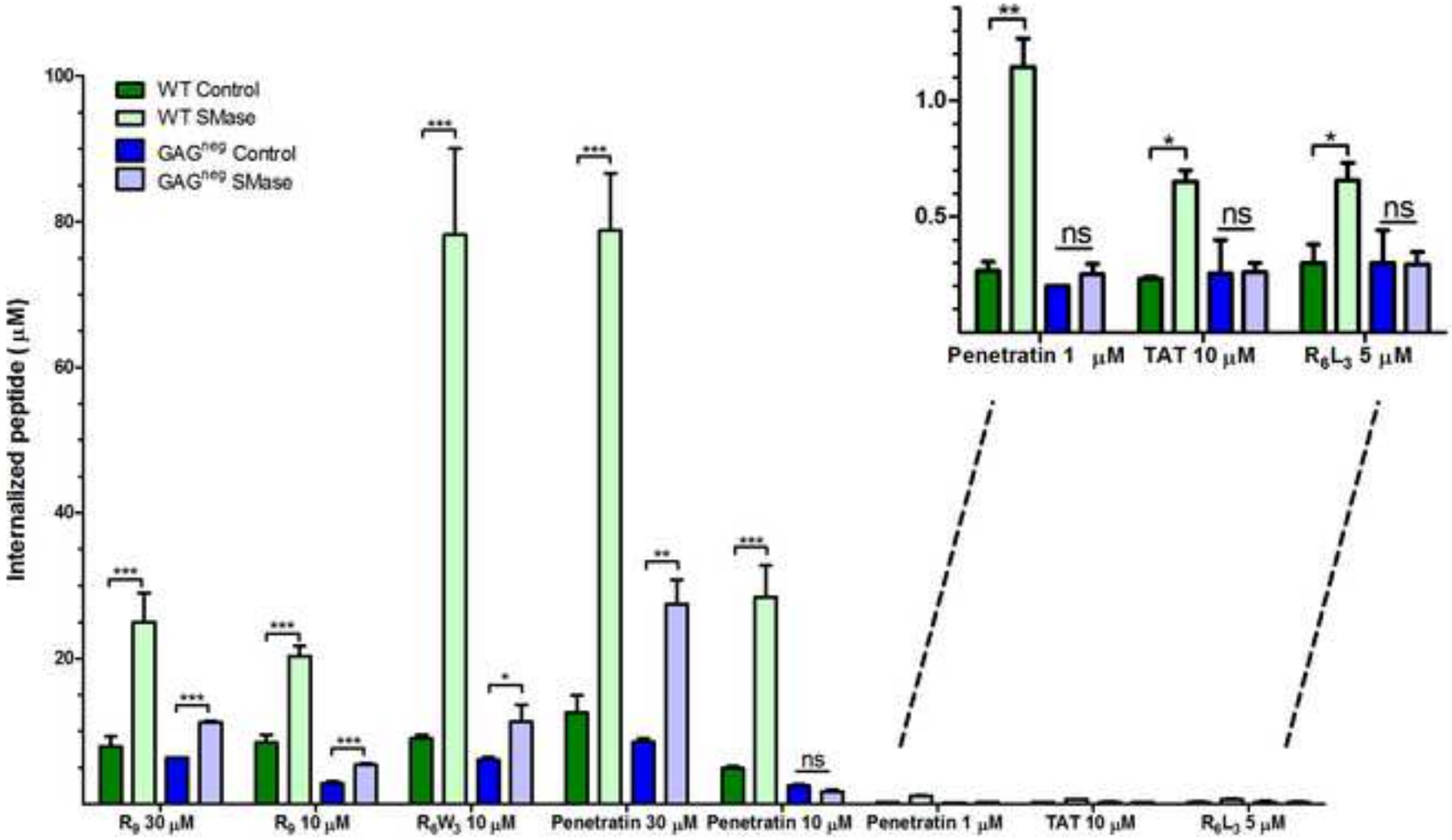

Figure 2
Click here to download high resolution image

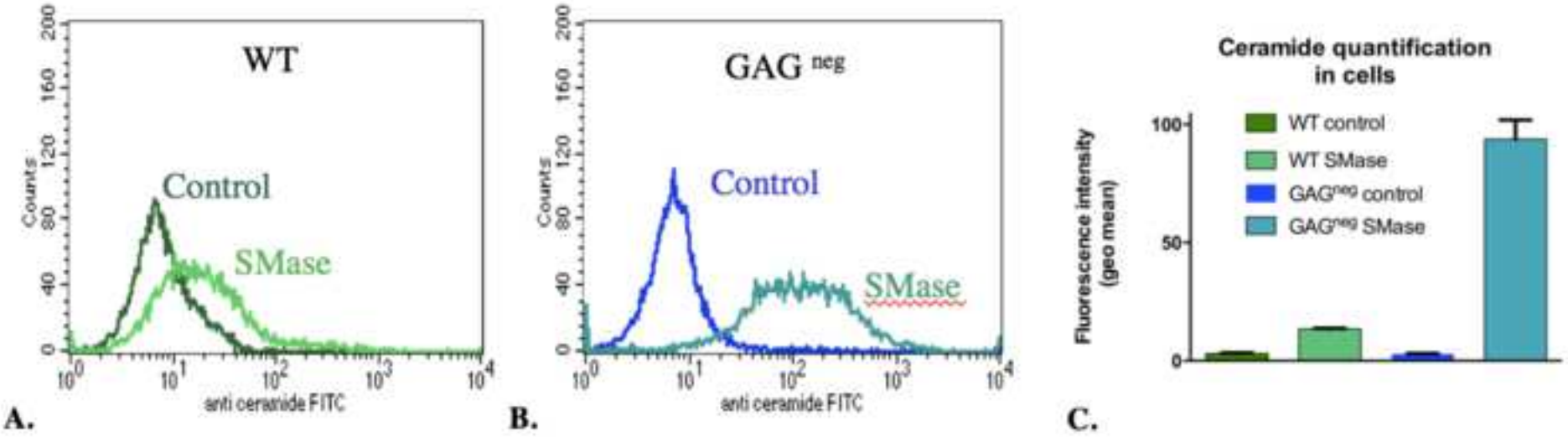

Figure 3
Click here to download high resolution image

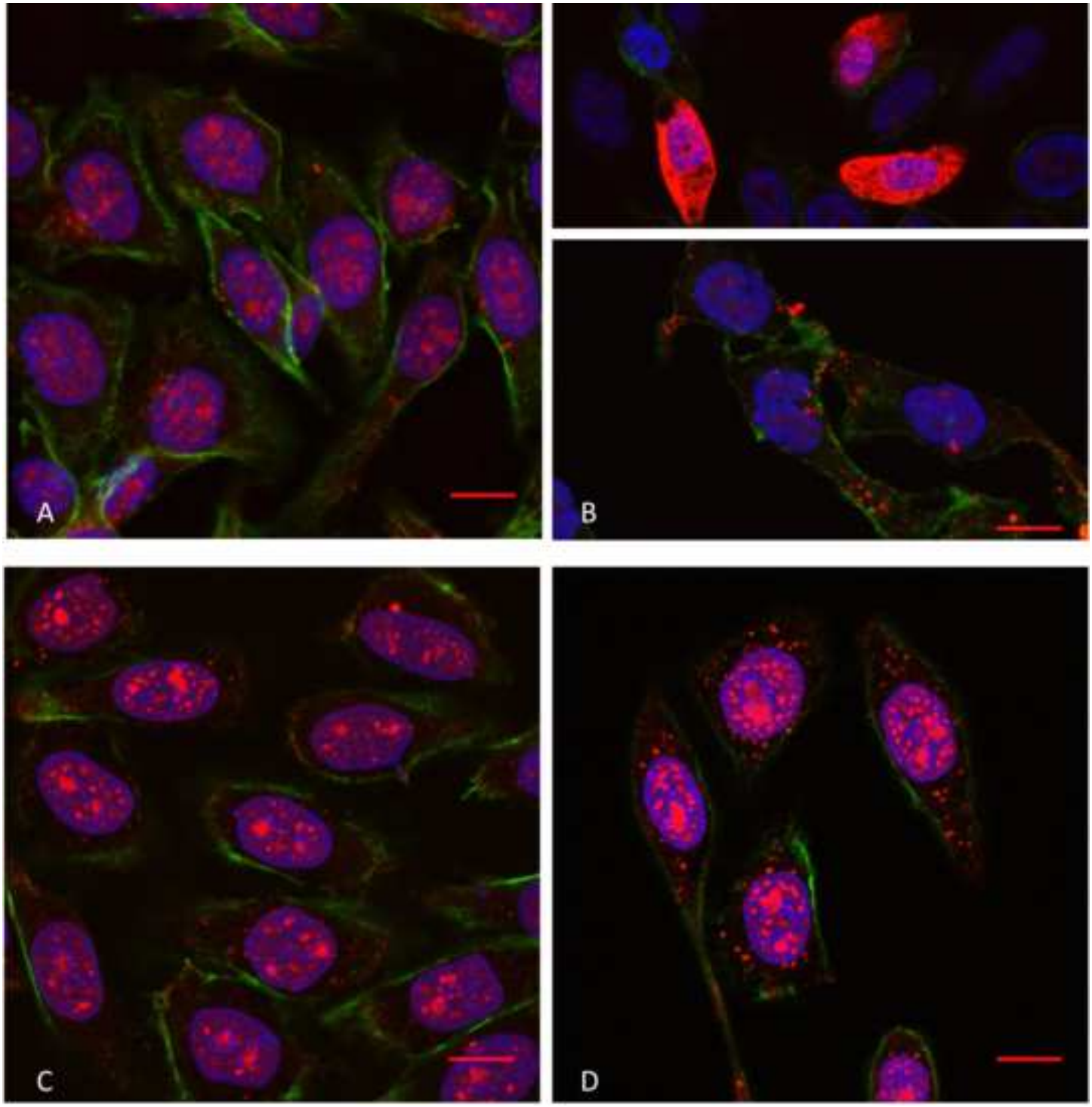

Figure 4
Click here to download high resolution image

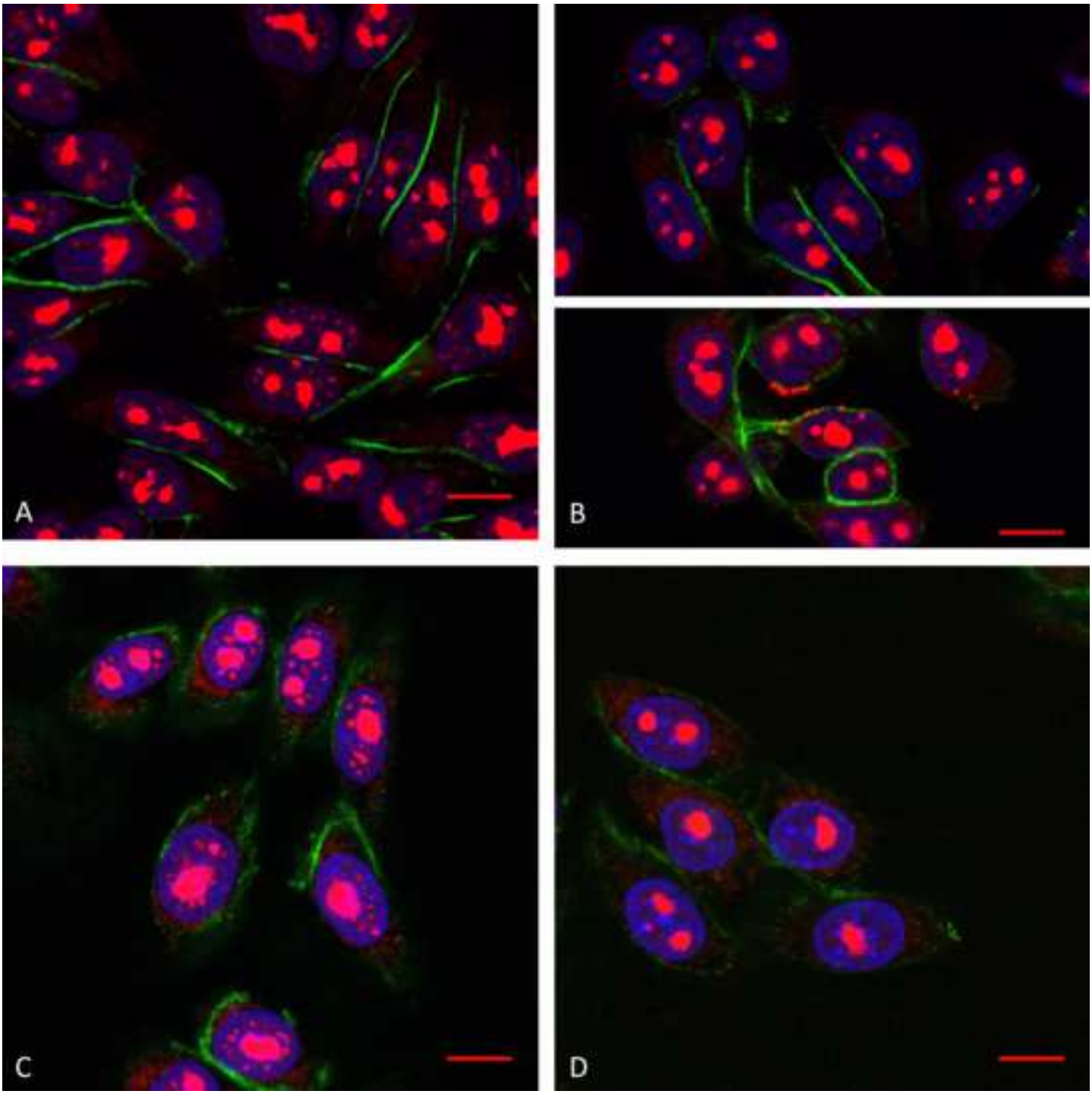

Figure 5
Click here to download high resolution image

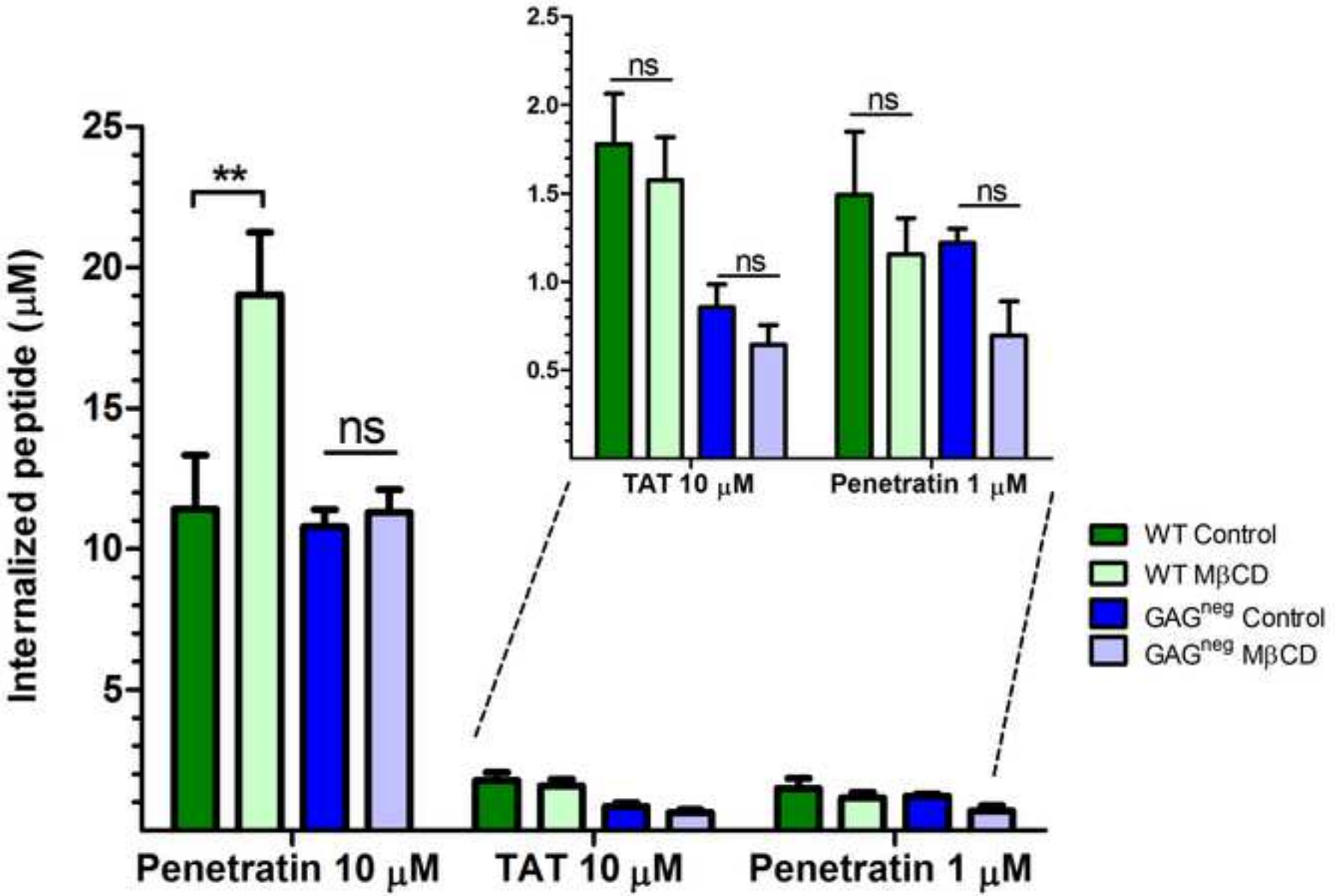

Figure 6
Click here to download high resolution image